Research Journal of Chemical Sciences _____ ISSN 2231-606X
Vol. **5(9),** 1-10, September **(2015)** *Res. J. Chem. Sci.*

Characterization, AC Impedance Study and Dielectric Properties of Chemically Synthesised Poly Para-Toluidine

Gopichand Madhusudhana and Jayasanthi Raj
PG and Research Department of Chemistry, Auxilium College, Vellore, Tamil Nadu 632006, INDIA

Available online at: www.isca.in, www.isca.me
Received 2nd July 2015, revised 4th August 2015, accepted 7th September 2015

Abstract

The present work is an investigation of AC impedance behaviour of Poly (para-toluidine). The polymer was synthesized by oxidative chemical polymerization of para toluidine in aqueous HCl using potassium dichromate as an oxidant at 0–3°C. The synthesized polymer was characterized by UV-VIS-NIR, FT-IR, XRD, SEM, and their thermal studies were carried out using TGA and DTA. The AC conductivity and dielectric behavior were investigated at a temperature varying from 298 to 373 K in the frequency varying from 20 Hz to 10^6 Hz. The AC conductivity increases as temperature is increased. In the entire range, the universal power law $\sigma_{ac}\omega = A\omega^S$ *holds well. The polymer displays a decrease in frequency exponent 'S' value in the entire temperature range of study and hence follow Correlated Barrier. As frequency decreases dielectric constant and dielectric loss increases exhibiting strong interfacial polarization at low frequency and the dissipation factor also decreases with frequency. At higher frequencies it exhibits almost zero dielectric loss which suggests that this polymer is lossless material at frequencies beyond 10^5Hz .Complex electric modulus exhibits two relaxation peaks, indicating two-phase structure as indicated by a bimodal distribution of relaxation process.*

Keywords: Poly (para-toluidine), conducting polymer, AC Impedance, dielectric behavior, dissipation factor.

Introduction

Polymers are generally insulators but few exhibit electrical conductivity when they possess ordered conjugation with extended π electrons and large carrier concentrations[1]. Conductive polymers with polyaromatic skeleton including polypyrrole, polythiophene, polyaniline, polytoluidine etc., have been researched extensively in the past few decades[2]. The conducting nature of these polymers can be controlled by the addition of dopant which can be carried out through an electro chemical synthesis, chemical synthesis, or photochemical route during which charge transfers from dopant to polymer or vice versa[1]. On addition of dopant these conjugated polymers exhibit conductivity comparable to metals because of which they are sometimes referred to as Synthetic Metals. They combine the conducting properties of metals with the advantage of polymers viz., lighter weight, higher workability, anticorrosive property and reduced cost. The most exciting applications of conductive polymers are in small screen sets, cellular telephones, automotive dashboard displays, Light Emitting Devices (LEDs), solar cells, lightweight batteries, polymer actuators, corrosion protection agents, sensors and molecular electronic devices[1,2]. Studies on undoped and weakly doped PANI and its derivatives POT, OPEA were explained in terms of polarons and bipolarons and their role towards conductivity and dielectric relaxation were studied by Nicholas et al[3].

Impedance spectroscopy is a very useful procedure in solid state electronic system, since it can determine the conduction components by distinguishing the transport properties of complex systems[3]. The dependence of AC conductivity on frequency and temperature usually follows a comparable activity in all disordered solids. Initially the alternating electric field applied to the material will induce transition of charges on deep or shallow defect centers. After this, they could migrate to long range or short range distance in the material. AC conductivity will be influenced by temperature variation specifically at long range distance where charges have time to be influenced by it[4,5].

Dielectric spectroscopy is a customary tool for examining the electrical response of substances involving conductivity and dielectric polarization. While studies of dielectric function in the microwave and far infrared frequencies explore the inter band excitations near the Fermi level, dielectric loss measurements using impedance spectroscopy investigates localized charge movements in nanometer range[6–8]. Most of the past studies have focused on examining the dielectric property of PANI and its derivatives at or below room temperature[7–13]. Young etal[13] have studied dielectric property of PANI in the radiofrequency range and fixed the AC conductivity versus temperature and frequency data with various theoretical models to arrive at the most probable conduction mechanism displayed by the system. Mathai et al[12] reported the dielectric activity of PANI film synthesized by AC plasma polymerization procedure up to 100°C and analyzed the increase in permittivity and loss tangent with increase in temperature based on a phenomenological lR–C circuit model. Lee et al have in detail studied the AC-conductivity of N-methylpyrrolidinone (NMP) plasticized PANI films in the temperatures varying from 50° to 250°C using

dielectric study. Proof for two relaxation peaks was also studied by Bengoechea et al[11] for NMP-plasticized films.

In the present work, poly (para-toluidine) (PPT) was synthesized by chemical oxidation method and characterized by different spectroscopic techniques. An attempt has been made to investigate the AC conductivity and dielectric behavior of PPT. Interesting results are observed from frequency and temperature-dependent AC conductivity and dielectric response of the polymer.

Material and Methods

Materials: The monomer Para-toluidine, p-toluene sulfonic acid, potassium dichromate, hydrochloric acid, were purchased as analytical grade and used as received without any further treatment.

Synthesis of poly (para-toluidine): Reagent grade p-toluidine was used to synthesize poly (para-toluidine). An aqueous 0.1M p-toluene sulfonic acid was prepared using double distilled water. Addition of 0.1M p-toluidine dissolved in 0.1M HCl, was made in a bath cooled by ice and salt mixture. Addition of Freshly prepared solution of 0.1M Potassium dichromate was done (to avoid warming) with constant stirring. The temperature was maintained below 5°C by ice and salt bath and to ensure that the reaction was completed it was stirred continuously for 2 h. The resultant polymer was repeatedly washed, filtered and dried[14].

Characterization: The FT-IR measurement of the polymer sample was carried out by compressing with KBr and recorded using Thermo Nicolet, Avatar 370 Spectrophotometer. UV VIS-NIR spectrum of PPT was taken by dissolving the sample in DMSO solvent and was obtained using Varian, Cary-5000 spectrophotometer in the range of 200–2500 nm. Thermo gravimetric analysis (TGA) measurements were carried out using a Schimadzu TGA-50 Japan system under a nitrogen atmosphere with a heating rate of 20^{o}C/ min with nitrogen as the purge gas. X-ray diffraction (XRD) scan was done with Bruker AXS D8 Advance Diffractometer at room temperature using Cu Kα (λ = 1.5406 ˚ A) with the 2θ angle ranged from 0° to 70°.

The dielectric studies were carried out in the temperatures varying from 298 to 373K by the complex impedance method. The study was carried out on the powder sample, which was previously made into circular pellets of 8mm diameter at a pelletizing pressure of 5 ton cm^{-2}, using a Hewlett Packard model HP 4284A Precision LCR Meter in the frequency range 20Hz to 10^6 Hz by inserting the sample pellet in between two silver electrodes. Complex impedance and modulus spectral formalisms were used for the analysis of these data. The electrical conductivity (σ_{ac}) of the polymer was estimated using the relationship

$$\sigma_{ac} = \frac{t}{Rb.A} \quad (1)$$

Where t is the thickness of the sample, A is the area of cross section, and R_b is the bulk resistance of the sample.

Results and Discussion

Fourier Transform infrared spectroscopy: The representative FT-IR spectrum of PPT is shown in figure-1. The broad peak at 3425-1800 cm^{-1} corresponds to stretching of aromatic C–H and –NH– groups, the bands at 1604cm^{-1} is attributed to a mixture of the C=C and C=N stretching vibrations in the quinoid ring, whereas the peak at 1481 cm^{-1} is assigned to the C=C stretching vibrations in the benzenoid ring. The peak at 1638 cm^{-1} shows the substitution for poly (p-toluidine) monomer unit at 1, 4 positions. The peak at 1276 cm^{-1} is assigned to the C–N stretching vibrations of the second aromatic amine, which shows the formation of a C–N–C structure in the polymer[14,15].

UV VIS-NIR Spectroscopy: The UV Vis-NIR spectrum of polymer was recorded in DMSO is shown in figure-2. The absorption band in the polymer appeared at 276nm is assigned to the π-π^* transition of the benzenoid ring which is related to the extent of conjugation between the phenyl rings along the polymeric chain. The absorption bands at 440nm corresponds to n-π*transitions and insulating pernigraniline phase of the polymer[14].

Thermal studies and Kinetic Parameters: TGA results show that the polymer degrades in three stages at 77^{0}C, 290^{0}C, and 490^{0}C as in figure-3. The initial stage of weight loss is due to the loss of water molecules/moisture, volatilization of the solvent and absorbed HCl present in the polymer matrix. The next stage weight loss is associated with the loss of the oligomers and dopants from the polymer matrix (dedoping). The final weight loss is due to the entire degradation and decomposition of the polymer backbone[16,17]. DTA studies show that the decomposition of PPT has taken place exothermally as is evident from the figure-4.

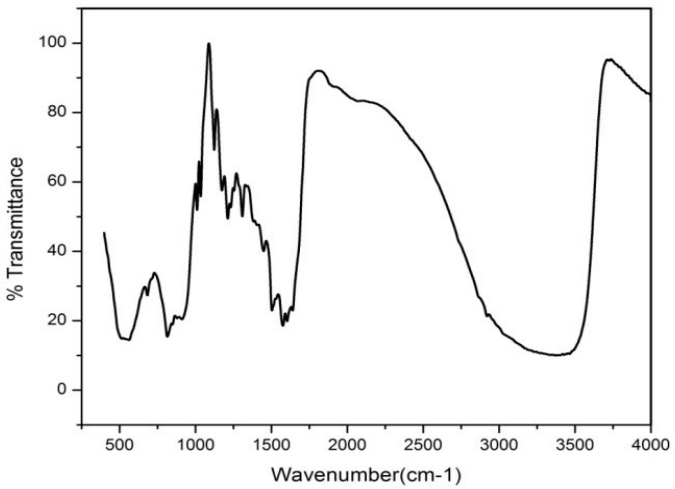

Figure-1
FT-IR spectra of PPT

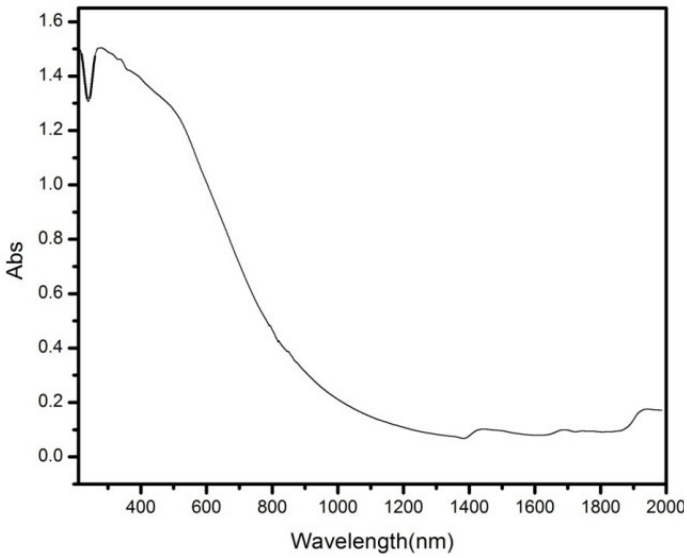

Figure-2
UV-VIS-NIR spectra of PPT

The first exothermic peak at 42.5^{0}C in the DTA curve is associated to the loss of absorbed HCl and moisture. The endothermic peak at 128 and 518^{0}C can be due to the loss of dopants, morphological changes and disruption of inter- and intra-molecular hydrogen bonding. The second broad exotherm signifies the final degradation step that occurs around 518^{0}C.

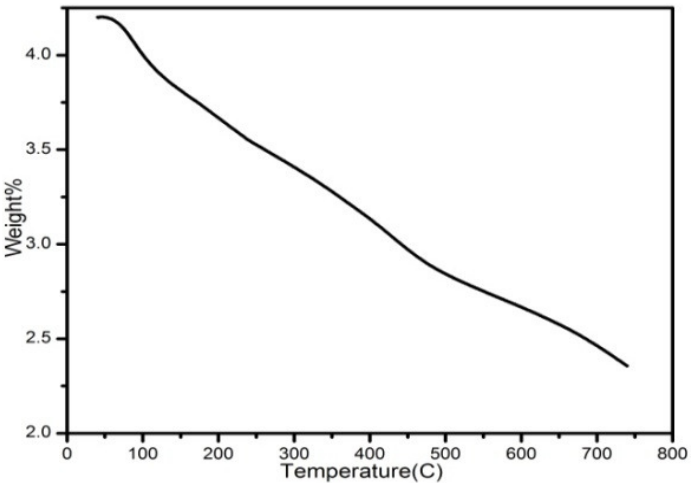

Figure-3
TGA of PPT

Thermal degradation kinetic parameter was calculated from TGA curves using Coats-Redfern[18] and Broido's[19,20] methods. For calculations and to study the nature of the decomposition, the complete thermo gram was separated into distinct sections according to their degradation processes. Coats-Redfern (CR) relation is

$$log\left(\frac{-\log(1-\alpha)}{T^2}\right) = \left(log\left(\frac{AR}{\beta E_a}\right)\right) - \left(\frac{E_a}{2.303RT}\right) \qquad (2)$$

Where α is the fraction of sample decomposed at temperature T, T is the derivative peak temperature, A is the frequency factor, β is the heating rate, Ea is the activation energy, and R is the gas constant.

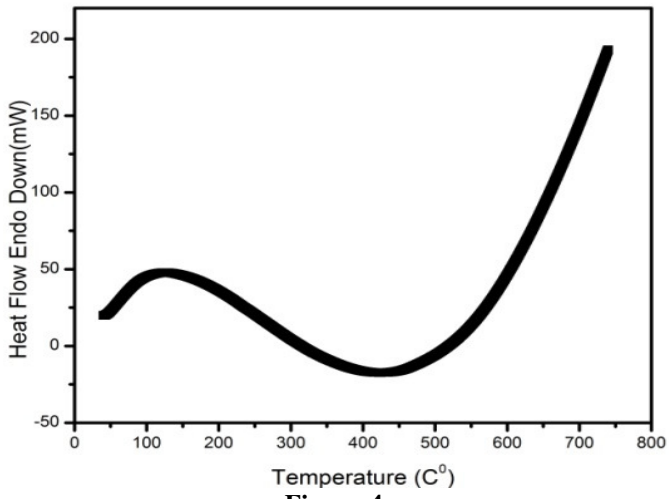

Figure-4
DTA of PPT

The Mathematical expression of Broido's (BR) method is given as:

$$log\left(-\log((1-\alpha)\right) = -\left(\frac{\mathrm{E_a}}{2.303\mathrm{RT}}\right)\left(\left(\frac{1}{\mathrm{T}}\right) + \mathrm{K}\right) \qquad (3)$$

Where $(1-\alpha)$ is the fraction of number of initial molecules not yet decomposed and T is the peak temperature of derivative curve of TGA. The plots of log $(-\log(1-\alpha)/T^2)$ versus $1/T$ (CR) and log $(-\log(1-\alpha))$ versus $1/T$ (BR) for PPT are depicted in Figures 5 and 6, respectively. The plots follow straight line whose slopes give the activation energy (Ea) of degradation process. The activation energies calculated by CR and BR methods are found to be 8.08 and 12.752 kJ/mol, respectively.

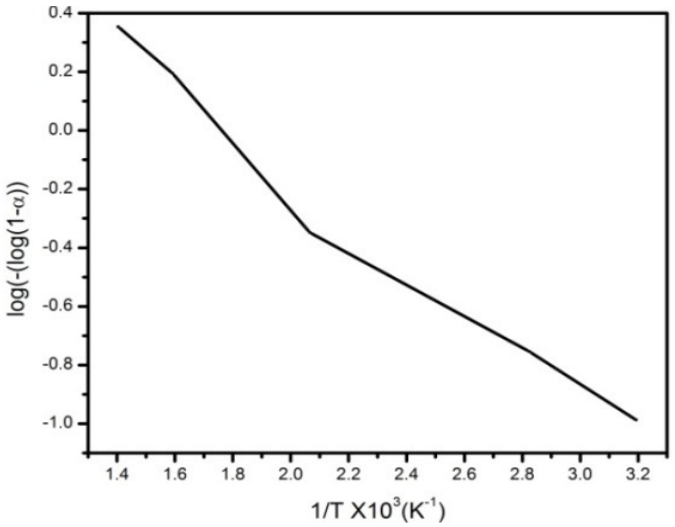

Figure-5
Plot of log $(-\log(1-\alpha)/T^2)$ versus $1/T$

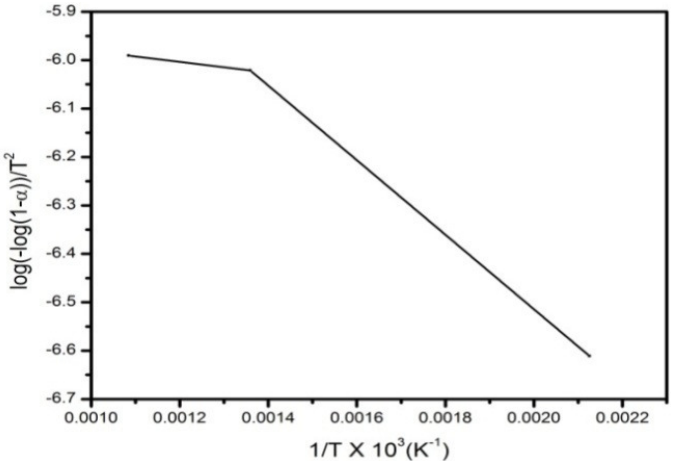

Figure-6
Plot of log (– log (1–α)) versus 1/T

XRD and SEM Analysis: It is observed that peaks obtained in the diffractogram patterns are discrete, sharp and intense as shown in figure-7. The sharp and intense peaks appearing at 21.518°, 24.04°, 30.451°, 19.53°, and 14.405° reveals the crystallinity of the polymer. The SEM photograph as shown in figure-8 reveals both crystalline and amorphous nature. The sharp edged particles and lamellar sides in crystalline regions were found to be intervened in the amorphous regions which consist of no definite shaped particles. This result was augmented from the X-ray diffractograms[21,22].

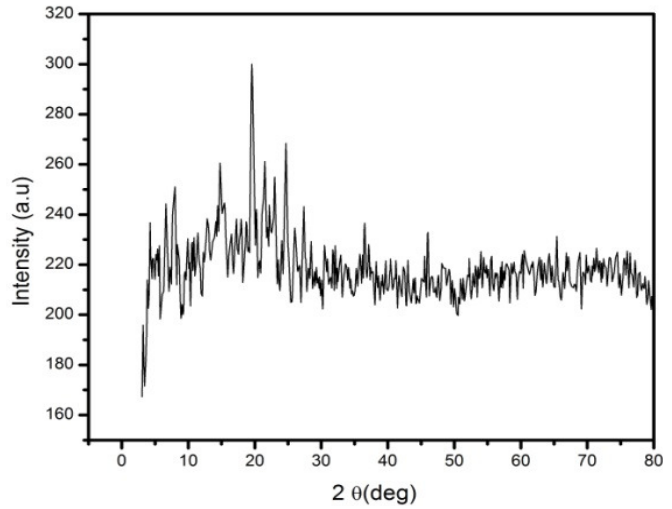

Figure-7
XRD pattern of PPT

AC Conductivity: It is a well established fact that frequency dependent complex conductivity results from interfacial polarization at grain boundaries, contacts, and other homogeneities in disordered materials such as polymers. The AC conductivity of insulator/conductor polymers has been compared to a resistance capacitance network, where the conducting dispersants are represented as resistors and the dielectric constant of the insulating matrix is represented by capacitors [23].The complex impedance plots for PPT measured at a temperatures range from 298 to 373K in the frequency region of 20 Hz to 10^6 Hz are shown in figure-9. The point of intersection of the impedance plot on the real axis gives the bulk resistance of the polymer. As temperature is increased this is shifted towards the origin as evident from figure-9, in other words, the intersection is found to shift towards higher frequency. Hence, it is evident that with the increase in temperature bulk resistance of the polymer decreases, resulting in the enhancement of electrical conductivity at higher temperatures.

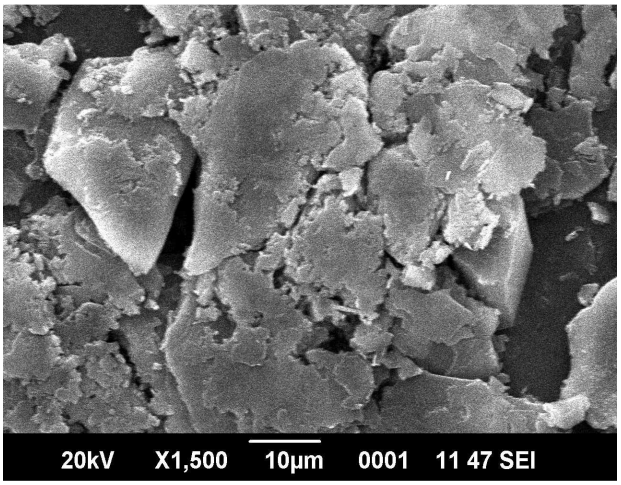

Figure-8
SEM micrograph of PPT

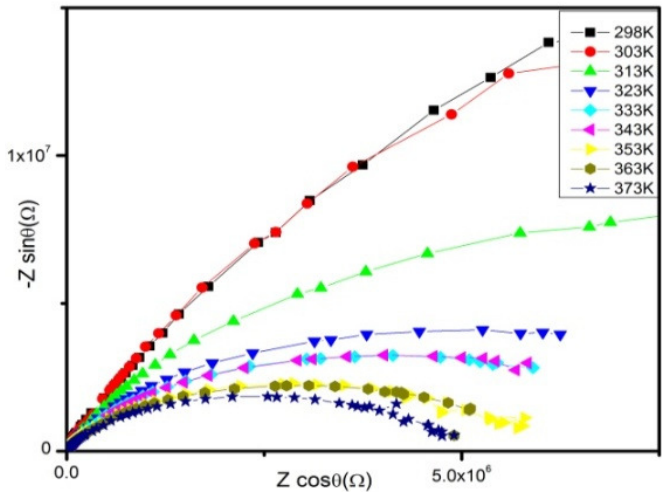

Figure-9
Complex impedance plots of PPT at different temperatures

The temperature-dependant conductivity value for PPT as in figure-10 reveals that the conductivity increases with temperature which is the distinctive feature of "thermal-activated behavior" owing to the amplified efficiency of charge transfer between polymer chains [25]. The temperature-dependent

conductivity data obtained for PPT over the temperature range 298 to 373 K are shown in figure-10, in the form of plots of logσT versus 1000/T where σ denotes the conductivity and T the absolute temperature. A remarkable phenomenon from figure-10 is that, as the temperature is increased electrical conductivity (σ) increases as in the case of polymers obeying the Arrhenius Relationship

$$\sigma T = \sigma_0 exp\left(-\frac{E_a}{RT}\right) \quad (4)$$

Where σ_0 denotes the pre exponential factor, Ea denotes the energy of activation for conduction, and K is the Boltzmann constant. From the slope of the linear plot drawn by the least square method the activation energy was calculated to be 0.2355 eV. The low activation energy for this polymer is attributed to the enhancement of the electronic jump between the localized states as found for other materials[26].

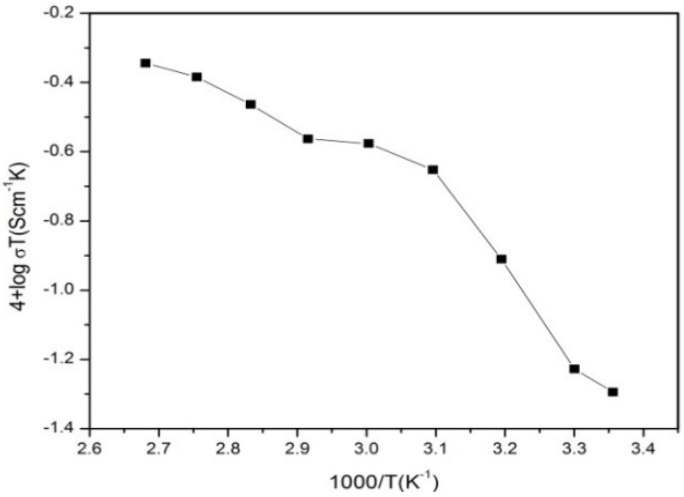

Figure-10
Temperature-dependent AC conductivity data of PPT

To investigate the nature of frequency-dependent AC conductivity, the plot of log (σ) versus log (ω) with in a frequency range 20Hz to 10^6 Hz over the temperature range 298 to 373K is drawn and the results are shown in figure-11. Many semiconductors, insulators, and inorganic and polymeric organic materials exhibit frequency-dependant electrical conductivity σ_{ac} (ω). Information about the electronic structure of such disordered materials can be found by charge transport measurements. Localization of electronic states or groups of states inside the material is due to disorder in atomic configuration and/or composition. Such behaviors caused by localized charge carriers are studied by AC impedance techniques[14].The fractional power dependence of the AC conductivity upon frequency has been observed in a wide variety of disordered materials, such as amorphous semiconductors, polymers and ionically conducting glasses [27-28]. The frequency dependence of the alternative current (AC) conductivity follows a power law behavior. σ' (ω) or the total AC conductivity can be represented by the following equation:

$$\sigma_0 = \sigma_{ac}(\omega) = \sigma_{dc} + A\omega^s \quad (5)$$

Where ω is the angular frequency, σ_{dc} is the independent frequency conductivity or DC conductivity, A is the constant dependent on temperature T, and S is an exponent dependent on both frequency and temperature with values in the range 0 to 1. AC conductivity in conducting polymers has been widely described by the power law Eq. (5) which originates from many-body interactions between the hopping charges[27,28]. In disordered systems such as conducting polymers, where hopping transport occurs, increase in frequency of the applied electric field increases the AC conductivity, due to short distance movements of charge carriers i.e., confined inside minuscule clusters and this type of behavior was studied by Jonscher, who called it the "Universal Dynamic Response" (UDR) [29] because wide variety of materials displayed such behavior.

A linear increase in conductivity with frequency is noticed and the value of the frequency exponent (S), estimated from the slope of the log (σT) versus log (ω), decreases with increase in temperature and is fully consistent with the power law as it is evident from the figure-11. The DC conductivity value presented in table-1 calculated by extrapolating the AC conductivity data to zero frequency region also shows an increase with increase in temperature.

According to the Correlated Barrier Hopping (CBH) model, the frequency exponent S values extend from 0.6 to1and decreases as temperature increases[31]. Our experimental results are in good agreement with this model suggesting that the electrical AC conduction mechanism of PPT at investigated temperature (298 to 373 K) can be explained by charge-carrier hops between sites over the potential barrier W_M separating them. The frequency exponent S for such model is given by the following equation-6[32].

$$S = \left(1 - \frac{6K_B T}{(W_M - KT(ln\omega_T))}\right) \quad (6)$$

Where W_M is the height of maximum barrier (or binding energy) and T is the relaxation time. W_M is calculated from the linear line slope which is between 1 – S and T. A value of W_M = 0.24 eV is obtained for PPT.

Determination of Dielectric Properties: The dielectric behavior of conducting polymers is one of the main focus points of research because of their novel technological applications. It is well established that the polymers, as dielectric materials, are excellent host matrices and also provide environmental and chemical stability.

The real part (ε') of the dielectric function (ε*) has been calculated from the measured values of capacitance using the following formula:

$$\epsilon' = \frac{C_d}{\varepsilon_0 A} \quad (7)$$

Where C is the measured capacitance of the sample, d is the thickness of the sample, A is the area of the pellet, and ε_o is the permittivity of free space. The imaginary part (ε") of the complex[34] impedance has been measured as

$$\epsilon'' = \epsilon' tan\partial \quad (8)$$

Where tan ∂ is the dissipation factor. Log (ε') figure-12 and log (ε") figure-13 vs log w depicts the variation of dielectric constant (ε') and dielectric loss (ε ") as a function of frequency for PPT in the temperature range of 293 to 373K.The dielectric constant of the PPT decreases moderately with frequency and increases with temperature[37]. As the frequency increases, the charge carriers migrating through the dielectric get trapped against a defect site and induce an opposite charge in its vicinity, as a result of which they slow down and the value of dielectric constant decreases moderately[35]. It is interesting to observe that the dependence of loss factor with the frequency of PPT decreases sharply with increase in frequency. The larger value of the loss factor or dielectric loss at low frequency could be due to the mobile charges within the polymer matrix. At high frequency, periodic field reversal is so fast that there is no excess ion diffusion in the direction of electric field[36]. Polarization due to charge accumulation decreases, leading to the decrease in the value of loss factor. Generally it is believed in dielectric analysis that the high frequency dielectric constant is mainly associated with dipolar relaxation, whereas at lower frequency and higher temperature, the contributions of interfacial polarization and DC conductivity become more significant in both ε' and ε". The difference in the dielectric relaxation time with change in concentration is due to the electric charges being displaced inside the polymer[38].

Table-1
Frequency exponent (*S*), conductivity of PPT

Temperature (K)	Frequency com ponent(S)	DC Conductivity (X10 -8Scm-1)
298	1.044	2.238
303	1.012	2.113
313	0.929	2.51
323	0.92	2.56
333	0.87	2.62
343	0.85	2.65
353	0.81	2.71
363	0.794	2.818
373	0.767	2.89

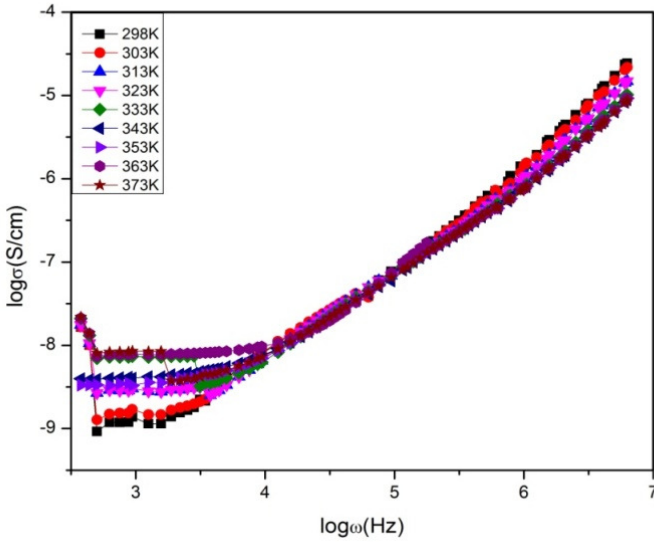

Figure-11
Frequency-dependent DC AC conductivity (log *σ* versus log *ω*)

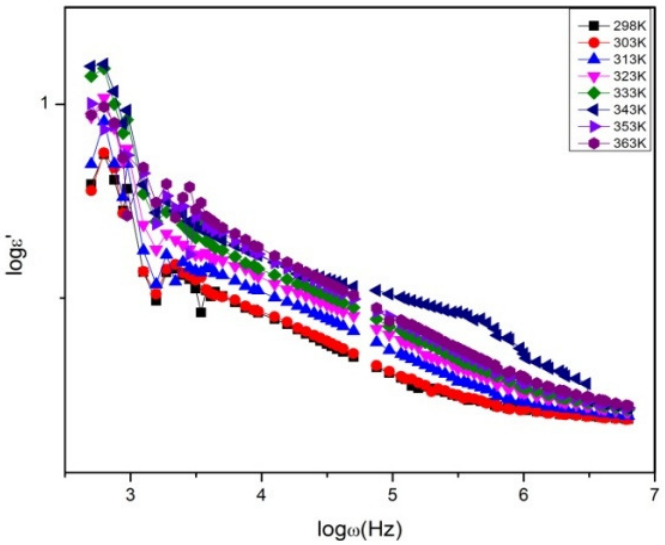

Figure-12
Logarithmic plots of dielectric constant as a function of frequency

For materials when charge carrier hopping is dominating in a conduction mechanism a typical phenomenon of strong low frequency (LF) dispersion for ε′ and ε″ is observed[39]. In the LF region, at higher temperatures the ε″ spectra exhibit no loss peaks and due to the increased contribution of DC conductivity it increases almost linearly with decreasing frequency. At low frequency the higher value of the loss factor or dielectric loss is due to the contribution of the mobile charges inside the polymer matrix[40]. At lesser temperatures and at a frequency around 10^3 Hz, a change in slope is observed in ε″ spectra as shown in Figure 13. Though there are no permanent dipoles in conducting polymers, when an external electric field is applied there is

strong charge (polaron) trapping and their localized (short range) motion serves as an "effective" electric dipole[34,39,40]. In presence of such an alternating electric field, dielectric relaxation results due to charge hopping among available localized site[41]. Due to the lack of strong pinning at low frequencies such charge hopping could extend all through the sample leading to a continuous current. At a given frequency, increase in temperature mobilizes the polymer chains, reduces pinning and leads to larger number of charges participating in the relaxation process. No relaxation mechanism can be noticed which may be attributed to shorter time constants associated with increased chain movement. However, it must be stated that efficient charge transport does not occur with increased chain movement since there is associated reduction in polymer conjugation at higher temperatures which increases the barrier potentials hindering charge transport. At higher temperatures, due to increased contribution of DC conductivity the change in slope due to dielectric relaxation is not observed. Generally it is believed in dielectric analysis, dielectric constant at high frequency is mainly associated with dipolar relaxation, whereas at higher temperature and lower frequency, the contributions of interfacial polarization and DC conductivity become more significant in both ε'and ε"

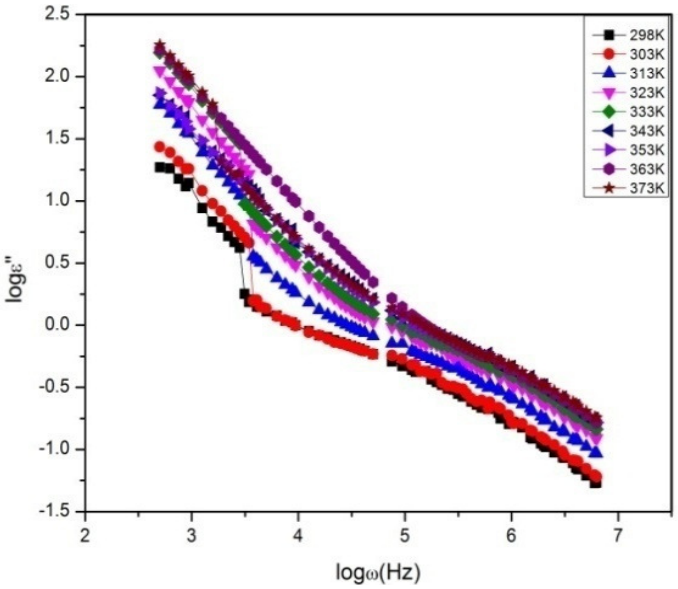

Figure-13
Logarithmic plots of dielectric loss as a function of frequency

PPT exhibits two peaks in isothermal as shown in figure-14 plot, indicating clearly two different relaxation processes. Due to the two-phase structure in the polymer two relaxation peaks may appear in isothermal plot. The peak observed at lower frequency can be attributed to the phase of oxidized repeat units (quinoid) and peak observed at higher frequency is due to the phase of reduced repeat units (benzenoid) of PPT [23]. It is seen from the frequency dependent M" plot that the frequency corresponding to $M"_{max}$ shifts to higher frequencies with increase in temperature[42]. It is observed that the isothermal peaks (figure-14) shift towards higher frequency when temperature is increased. The height of the peak corresponding to the relaxation of the reduced units (higher frequency) is significantly lower than the peak corresponding to the oxidized unit[43].

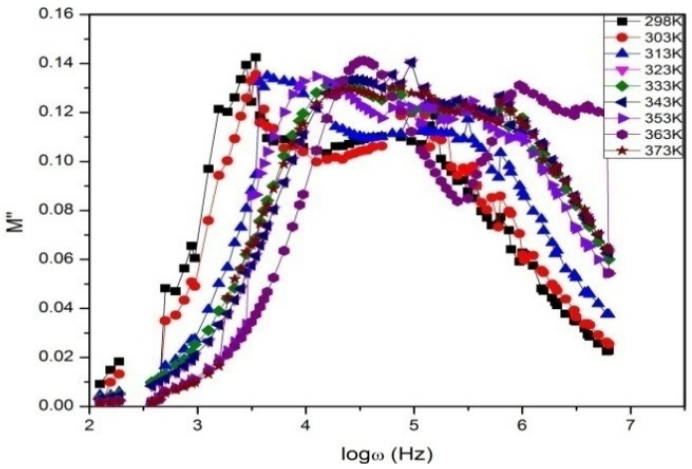

Figure-14
Isothermal dependence of ε" on the frequency for PPT

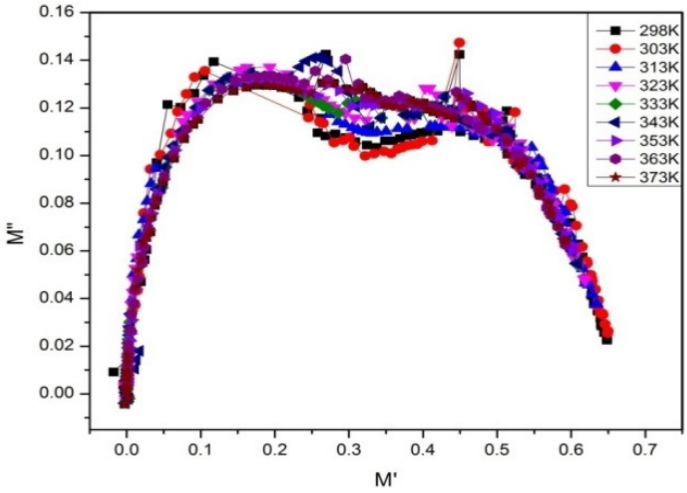

Figure-15
M' real part of electric modulus plotted against M" imaginary part of electric modulus for PPT

The imaginary part of electric modulus as given in figure-15 is plotted against the real part of the modulus for PPT and two arcs are exhibited in the figures which correspond to two relaxation processes. The arcs initiate from the origin and spread to different values of M" depending upon the temperature. The dissipation factor, tan∂ recorded as a function of frequency for PPT is shown in figure-16. The loss tangent decreases with increasing frequency[44]. As noted earlier, high loss at low frequency in loss tangent may be attributed to DC conduction losses as in the case of dielectric constant and dielectric loss.

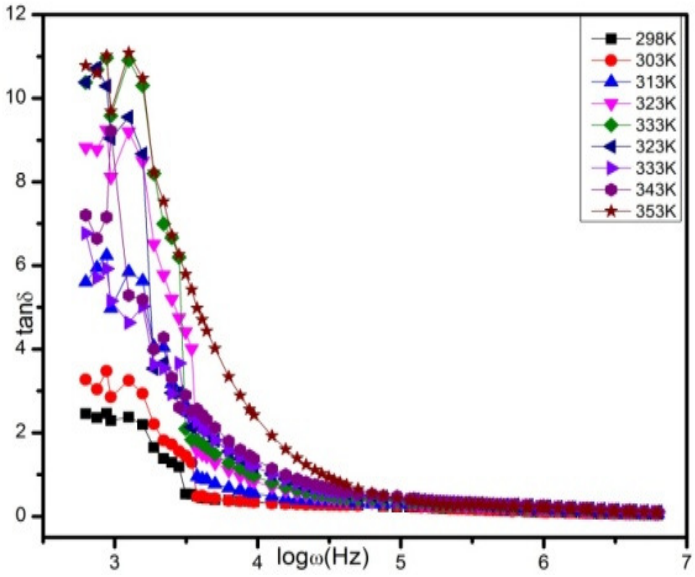

Figure-16
Frequency dependence of dissipation factor of PPT

At higher frequencies beyond 10^5 Hz, PPT exhibits almost zero dielectric loss which suggests that this polymer is lossless material at higher frequencies. Since the temperature at which the loss tangent peak occurs, increases with increasing frequency, it is evident that these peaks are due to thermally activated relaxation processes in the film. The two peaks at a given frequency correspond to two relaxation processes[45].

Conclusion

Poly (Para Toluidine) has been successfully synthesized by chemical oxidative polymerization method at 0–3°C and characterized by different spectroscopic techniques. The characterization by UV-VIS-NIR, FT-IR, suggests the formation of quinoid and benzenoid rings which confirmed the formation of polymer. The XRD and SEM studies reveal that the morphology of PPT is partially crystalline and amorphous in nature. It was observed from thermal analysis that PPT exhibits three-step decomposition patterns. The frequency dependent electrical parameters, such as impedance, AC conductivity, dielectric constant, dielectric loss, and electric modulus for PPT, have been studied within the range of 20 Hz to 10^6 Hz over the temperature ranging from 298 to 373K. With increase in temperature AC conductivity increases moderately and obeys the power law of frequency. The temperature variation of frequency exponent suggests that the behavior of AC conductivity can be described by CBH mechanism. The dielectric constant and dielectric loss decrease with an increase in frequency. The electric modulus and dissipation factor recorded as a function of frequency display two relaxation processes. At higher frequencies PPT exhibits low dielectric loss, which suggests that PPT is lossless material at frequencies beyond 10^5 Hz.

References

1. Shumaila G.B., Lakshmi V.S., Alam M., Siddiqui A.M., Zulfequar M. and Husain M., Synthesis and Characterization of Se Doped Polyaniline, *Current Applied Physics.*, **11(2)**, 217 **(2010)**

2. Gupta K., Jana P.C. and Meikap A.K, Optical and Electri-cal Transport Properties of Polyaniline-Silver Nanocomposite, *Synthetic Metals.*, **160(13)**, 1566 **(2010)**

3. Nicholas J. Pinto., Angel A., Acosta A., Ghanshyam P., Sinha B. and Fouad M. Aliev., Dielectric permittivity study on weakly doped conducting polymers based on polyaniline and its derivatives, *Synthetic Metals.,* **113**, 77 **(2000)**

4. Nadeem M., Akhtar M.J. and Haque M.N., Increase of grain boundary resistance with time by impedance spectroscopy in La0.50Ca0.50MnO3+δ at 77 K, *Solid State Communications.*, **145(5-6)**, 263 **(2008)**

5. Akgul U., Ergin Z., Sekerci M. and Atici Y., AC conductivity and dielectric behavior of [Cd (phen)2 (SCN)2], *Vacuum.*, **82(3),** 340 **(2007)**

6. Singh R., Kumar J., Singh R.K., Kaur A., Sinha R.D.P. and Gupta N.P., Low frequency AC conduction and dielectric relaxation behavior of solution grown and uniaxially stretched poly (vinylidene fluoride) films, *Polymer.*, **47(16),** 5919 **(2006)**

7. Capaccioli S., Lucchesi M., Rolla P.A. and Ruggeri G., Dielectric response analysis of a conducting polymer dominated by the hopping charge transport, *J. Phys.: Condens. Matter.*, **10,** 5595 **(1998)**

8. Mathai C.J., Sarvanan S., Anantharaman M.R., Venktichalam S. and Jayalekshmi S, Conduction mechanism in plasma polymerised aniline thin film, *J Phys. D Appl. Phys.,* **35**, 240 **(2002)**

9. Sakellis I., Papathanassiou A.N. and Grammatikakis J., Effect of composition on the dielectric relaxation of zeolite-conducting polyaniline blends, *J. Appl. Phys.,* **105**, 064109 **(2009)**

10. Papathanassiou A.N., Grammatikakis J., Sakellis I., Sakkopoulos S., Vitoratos E. and Dalas E., Effect of composition on the dielectric relaxation of zeolite-conducting polyaniline blends, *J. Appl. Phys.,* **96,** 3883 **(2004)**

11. Bengoechea M.R., Aliev F.M. and Pinto N.J, Investigation of Electrical Properties of Polyaniline Nanocomposites by Impedance Spectroscopy, *J. Phys. Condens. Matter.,* **14,** 11769 **(2002)**

12. Papathanassiou N., Sakellis I., Grammatikakis J., Vitoratos E., Sakkopoulos S. and Dalas E., Low frequency A. C. conductivity of fresh and thermally aged polypyrrole–polyaniline conductive blends, *Synth. Me. t,*

142, 81 **(2004)**

13. Hsun-Tsing Lee, Kuen-Ru Chuang, Show-An Chen, Pei-Kuen Wei, Jui-Hung Hsu and Fann Wunshain, Conductivity Relaxation of 1-Methyl-2-pyrrolidone Plasticized Polyaniline Film, *Macromolecules.*, **28(23)**,7645 **(1995)**

14. Diaz Calleja R., Matveeva E.S. and Parkhutik V.P, Equivalent circuit analysis of the electrical properties of conducting polymers: electrical relaxation mechanisms in polyaniline under dry and wet conditions, *J Non-Cryst Solids.,***180**, 260 **(1995)**

15. Jyoti Kattimani, T. Sankarappa, Ramanna R. and Ashwajeet J.S., Frequency and Temperature dependence studies in PTh-V2O5 composites, *Research Journal of Chemical Sciences.,* **5(6),** 59-63 (**2015)**

16. Chen C., Sun C. and Gao Y, Electrosynthesis of poly(aniline co-p-aminophenol) having electrochemical properties in a wide pH range, *Electrochimica Acta.*, **53(7),** 3021 **(2008)**

17. Savitha P. and Sathyanarayana D.N., Copolymers of aniline with *o*- and *m*-toluidine: synthesis and characterization *Polym Int.*, **53**, 106 **(2004)**

18. Anand J., Palaniappan S. and Sathyanarayana D.N., In Handbook of Organic Conductive Molecules and Polymer, Nalwa, H.S., Ed., Wiley: Chichester, England., **2**, 573 **(1993)**

19. Coats A.W. and Redfern J.P., Kinetic parameters from thermo gravimetric data, *Nature.*, **201,** (4914)68 **(1964)**

20. Broido B.A., A Simple, sensitive graphical method of treating thermo gravimetric analysis data, *Journal of Polymer Science A.*, **7(10**), 1761 **(1969)**

21. Archana S. and Jaya Shanthi R, Synthesis and Characterization of Poly (p-phenylenediamine) in the Presence of Sodium Dodecyl Sulfate, *Research Journal of Chemical Sciences*, **4(2)**, 60-67 **(2014)**

22. Sh. M., Ebrahim Gad A. and Morsy A., Highly crystalline and soluble dodecyl benzene sulfonic acid doped poly(o-toluidine), *j. Synthmet.,* **10**, 021 **(2010)**

23. Hasim Yilmaz 1, Halil Ibrahim Unal 2, Bekir Sari Synthesis, Characterization and Electro rheological Properties of Poly (o-toluidine) /Zn Conducting Composites, *Journal of Applied Polymer Science.,* **103,** 1058 **(2007)**

24. Ramesh Patil, Roy A.S., Anilkumar K.R, Jadhav K.M. and Shrikant Ekhelikar, Dielectric relaxation and AC conductivity of polyaniline-zinc ferrite composite, *Composites B.*, **43(8**) 3406 **(2012)**

25. Chithra Lekha P., Subramanian S. and Pathinettam Padiyan D., Investigation of pseudo capacitance effect and frequency dependence of AC impedance in Polyaniline-polyoxometalate hybrids, *Journal of Materials Science.*, **44(22)** ,6040 **(2009)**

26. Koteswara Rao K., Rambabu G., Raghavender M., Prasad G., Kumar G.S. and Vithal M., Preparation, characterization and impedance study of AgTaMP3O12 (M=Al, Ga, In, Cr, Fe and Y), *Solid State Ionics.,* **176,** 2701 **(2005)**

27. Seyam M.A.M., Bekheet A.E. and Elfalaky A., AC conductivity and dielectric properties of In2S3 films, *European Physical Journal*, **16(2),** 99 **(2001)**

28. Jonscher A.K., Dielectric relaxation in solids, Chelsea Dielectrics Press, London (**1983)**

29. Jager K.M, McQueen D.H., Tchmutin I.A., Ryvkina N.G. and Kluppel M., Electron transport and AC electrical properties of carbon black polymer composites, *J. Phys. D: Appl. Phys.,* **34,** 2699 **(2001)**

30. Jonscher A.K., The universal dielectric response, *Nature.*, **267**, (5613) 673 (**1977)**

31. Long A.R., Frequency-dependent loss in amorphous semiconductors, *Adv Phys.*, **31(5)** 553 (**1982)**

32. Gudmundsson J.T., Svavarsson H.G, Gudjonsson S. and Gislason H.P., Frequency-dependent conductivity in lithium diffused and annealed GaAs, *Physica B.*, **340,** 324 **(2003)**

33. Kahouli A., Sylvestre A., Jomni F., Yangui B. and Legrand J., Experimental and theoretical study of AC electrical conduction mechanisms of semi crystalline parylene C thin films, *Journal of Physical Chemistry A.*, **116(3)**, 1051 **(2012)**

34. Singh N. and Khanna P.K., In situ synthesis of silver nano particles in poly methyl methacrylate, *Materials Chemistry andPhysics.***, 104(2)**, 367 **(2007)**

35. Papathanassiou A.N., Grammatikakis J., Sakkopoulos S., Vitoratos E. and Dalas E., Localized and long-distance charge hopping in fresh and thermally aged conductive copolymers of polypyrrole and polyaniline studied by combined TSDC and DC conductivity, *J. Phys. Chem. Solid. S*, **63**, 1771 **(2002)**

36. Suresh S., Optical and Dielectric Properties of L-Histidinium Trifluoroacetate NLO Single Crystal, *Research Journal of Chemical Sciences.,* **2(2),** 83-86 **(2012)**

37. Bhargav P.B., Sarada B.A., Sharma A.K. and Rao V.V.R.N., Electrical conduction and dielectric relaxation phenomena of PVA based polymer electrolyte films, *Journal of Macromolecular Science A.*, **47(2)**, 131 **(2010)**

38. Jyoti Kattimani, Sankarappa T., Ramanna R. and Ashwajeet J.S, Frequency and Temperature dependence studies in PTh-V2O5 composites, *Research Journal of Chemical Sciences*, **5(6),** 59-63 **(2015)**

39. Bisquert J, Garcia-Belmonte G., Bueno P., Longo E. and Bulhoes L.O.S., Impedance of constant phase element (CPE)-blocked diffusion in film electrodes, *J Electroanal Chem.,* **452**, 229 **(1998)**

40. Chen S.A. and Liao C.S., Conductivity relaxation and chain motions in conjugated conducting polymers: neutral poly (3-alkylthiophenes) *Macromo.l,* **26**, 2810 **(1993)**

41. Bhargav P.B., Sarada B.A., Sharma A.K and Rao V.V.R.N., Electrical conduction and dielectric relaxation phenomena of PVA based polymer electrolyte films, *Journal of Macro molecular Science A.*, **47(2)**, 131 **(2010)**

42. Zuo F., Angelopolous M., MacDiarmid A.G. and Epstein A., AC conductivity of emeraldine polymer, *J. Phys. Rev. B.,* **39**, 3570 **(1989)**

43. Amrtha Bhide and Hariharan K., Ionic transport studies on (PEO)6:NaPO3 polymer electrolyte plasticized with PEG400, *European Polymer Journal.*, **43**, 4253 **(2007)**

44. Thenmozhi Gopalasamy, Mohanraj Gopalswamy, Madhusudhana Gopichand and Jayasanthi Raj, Poly Meta-Aminophenol: Chemical Synthesis, Characterization and AC Impedance Study, *Journal of Polymers.*, Article ID **827043**, 11 **(2014)**

45. Solanki G.K, Patel K.D, Gosai N.N. and Patel Rahul B, Growth and Dielectric Properties of $SnSe0._5Te0._5$ Crystals, *Res. J. Chem. Sci.,* **2(10),** 43-48 **(2012)**

46. Ashwini N. Mallya, Yashavanth Kumar G.S., Rajeev Ranjan and Praveen C. Ramamurthy, Dielectric relaxations above room temperature in DMPU derived polyaniline film, *Physica B.,* **407**, 3828 **(2012)**